

Computational Supremacy of Quantum Eigensolver by Extension of Optimized Binary Configurations

Hayun Park¹ and Hunpyo Lee^{1,2,*}

¹*Department of Liberal Studies, Kangwon National University, Samcheok, 25913, Republic of Korea*

²*Quantum Sub Inc., Samcheok, 25913, Republic of Korea*

(Dated: June 6, 2024)

We developed a quantum eigensolver (QE) which is based on an extension of optimized binary configurations measured by quantum annealing (QA) on a D-Wave Quantum Annealer (D-Wave QA). This approach performs iterative QA measurements to optimize the eigenstates $|\psi\rangle$ without the derivation of a classical computer. The computational cost is ηML for full eigenvalues E and $|\psi\rangle$ of the Hamiltonian \hat{H} of size $L \times L$, where M and η are the number of QA measurements required to reach the converged $|\psi\rangle$ and the total annealing time of many QA shots, respectively. Unlike the exact diagonalized (ED) algorithm with L^3 iterations on a classical computer, the computation cost is not significantly affected by L and M because η represents a very short time within 10^{-2} seconds on the D-Wave QA. We selected the tight-binding \hat{H} that contains the exact E values of all energy states in two systems with metallic and insulating phases. We confirmed that the proposed QE algorithm provides exact solutions within the errors of 5×10^{-3} . The QE algorithm will not only show computational supremacy over the ED approach on a classical computer but will also be widely used for various applications such as material and drug design.

PACS numbers: 71.10.Fd, 71.27.+a, 71.30.+h

Introduction—Fast computation to find the full eigenvalues E and eigenstates $|\psi\rangle$ of a Hermitian matrix \hat{H} of size $L \times L$ is a highly desirable technique which has been widely applied across various applications, including many-body electronic systems, electronic structures, novel material design and drug design. The full values of E and $|\psi\rangle$ can be computed using an exact diagonalization (ED) method, where the computational cost demands iterations of L^3 on a classic computer based on bits [1]. Another approach using a classic computer is to employ an optimization approach. The lowest eigenvalue E^{Lowest} and its $|\psi\rangle$ can be determined using the optimization equation $E^{\text{Lowest}} = \min_{|\psi\rangle} \langle \psi | \hat{H} | \psi \rangle$, where $|\psi\rangle$ retains continuous variables. A gradient descent (GD) method is then employed to solve the continuous-variable optimization problem. The computational cost for determining E^{Lowest} and its $|\psi\rangle$ requires the derivation of $N \times L$, where N is the number of iterations required to reach the converged E^{Lowest} . N generally increases with L . The excited eigenvalue and eigenstate are also computed using the same optimization method with the constraint of the orthonormal condition between the eigenstates. The overall computational cost for determining the full E and $|\psi\rangle$ in all the energy states is approximately $N^2 \times L^2$. Therefore, it is difficult to calculate the full E and $|\psi\rangle$ of \hat{H} with massive L in a feasible time using both ED and GD approaches on classic computer.

The variational quantum eigensolver (VQE) algorithm on gate-type quantum computers with qubit circuits is another promising tool for determining E^{Lowest} and its $|\psi\rangle$ of \hat{H} [2–4]. These are measured by the operation of qubits on a circuit in combination with derivations on a classical computer. Many degrees of freedom for express-

ing continuous variables $|\psi\rangle$ require a deep circuit, which is accompanied with large quantum errors. Therefore, another qubit is required to minimize the larger quantum errors. Present gate-type quantum computers are only composed of approximately hundreds of qubits, which is insufficient to reduce quantum errors for large \hat{H} , even though they show limitless possibilities with increasing qubits in the future [2].

The quantum annealing (QA) approach on adiabatic quantum computers is another alternative for fast computation of optimization problems [5–7]. The QA approach measures the possible $|\psi^{\text{Binary}}\rangle$ with only the optimized binary configurations through the quantum adiabatic process in the transverse-field Ising model, where $|\psi^{\text{Binary}}\rangle$ is the optimized binary spin configuration. This has already been performed on D-Wave quantum annealer (D-Wave QA) with 5000 qubits, which can compete with classic computers in terms of computational speed and accuracy for combinatorial optimization problems of moderate size [8, 9]. It can be also employed as quantum simulators for exploring phase transition and dynamic behaviors [10–17]. On the other hand, the method only works well on binary combinatorial optimization problems and is limited to continuous-variable optimization problems. Therefore, an extension of the approach to continuous-variable optimization problems that can be applied to more important applications is required in D-Wave QA.

In this Letter, we describe the development of a full quantum eigensolver (QE) that is based on the extension of optimized binary configurations determined using QA on the D-Wave QA. This method determines the possible E^{QE} and $|\psi^{\text{QE}}\rangle$ values with continuous variables in all

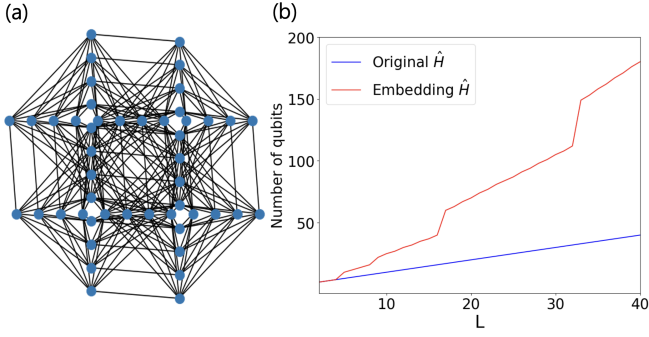


FIG. 1. (Color online) (a) Zephyr graph with 20 couplers between qubits on D-Wave QA Advantage2 prototype2.3. (b) Number of qubits as a function of L for embedding Hamiltonian \hat{H} required for quantum annealing measurement of the fully connected systems. The original \hat{H} means the topology without the chains.

energy states through iterative QA measurements. The computational cost is ηML for full E^{QE} and $|\psi^{\text{QE}}\rangle$ of \hat{H} of size $L \times L$, where M and η are the number of QA measurements required to reach the converged $|\psi\rangle$ and the total annealing time of many QA shots, respectively. This means that, because η is very short, L and the other parameters in \hat{H} do not significantly affect the computational time. We selected a one-dimensional (1D) ionic non-interacting tight-binding \hat{H} whose exact E is known in the entire energy spectrum. We measured the possible E^{QE} and $|\psi^{\text{QE}}\rangle$ in various cases of both metallic and insulating phases using our QE algorithm for D-Wave QA. We compared them with the exact E and confirmed that it provides an exact E within the errors of 5×10^{-3} . We believe that the proposed QE approach exhibits computational superiority over ED with L^3 iterations and GD with $N^2 L^2$ derivations on a classical computer.

Algorithm of Quantum Eigensolver (QE)— E^{Lowest} and its $|\psi\rangle$ of \hat{H} are determined by the optimization equation given as

$$E^{\text{Lowest}} = \min_{|\psi\rangle} \langle \psi | \hat{H} | \psi \rangle, \quad (1)$$

where $|\psi\rangle$ retains the continuous variable. The idea of our algorithm is to separate $|\psi\rangle$ into $|\psi\rangle = |\psi'\rangle + |\phi\rangle$. Both $|\psi'\rangle$ and $|\phi\rangle$ are determined by iterative QA measurements. The detailed computational procedure is followed as: (i) We first determine E' and $|\psi'\rangle$ in $E' = \min_{|\psi'\rangle} \langle \psi' | \hat{H} | \psi' \rangle$ by QA measurement. The initial $|\psi'\rangle$ is only expressed as possible $|\psi^{\text{Binary}}\rangle$ that shows very rough solution of the optimized binary configuration. (ii) We modify \hat{H} into $\hat{H} - E'I$, where I is the identity matrix. Now we rewrite $|\phi\rangle$ into $|\phi\rangle = |\psi\rangle - |\psi'\rangle$, and optimize $|\psi\rangle$ in $\hat{H} - E'I$. The optimization equation for $|\psi\rangle$ is given as

$$E_{|\psi\rangle} = \min_{|\psi\rangle} [(\langle \psi | - \langle \psi' |) \hat{H}^{(ii)} (|\psi\rangle - |\psi'\rangle)], \quad (2)$$

where $\hat{H}^{(ii)}$ is $\hat{H}^{(ii)} = \hat{H} - E'I$. $|\psi'\rangle$ were already known

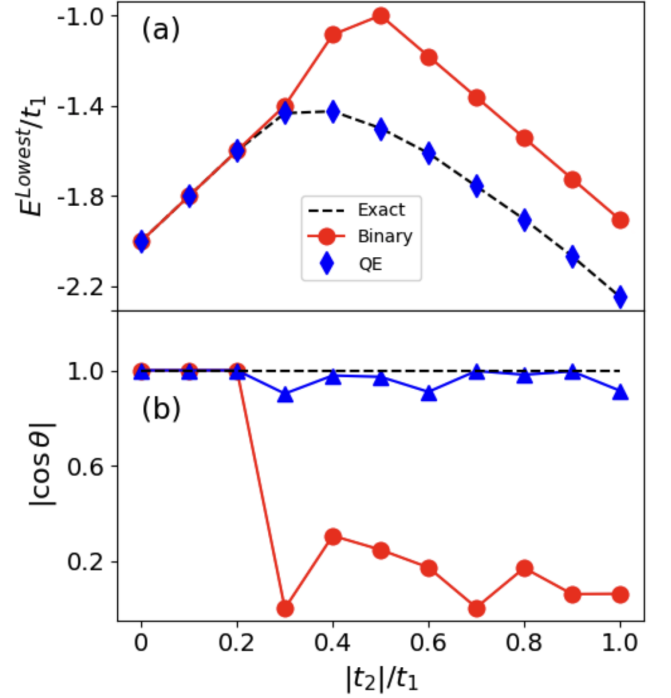


FIG. 2. (Color online) (a) The lowest eigenvalues E^{Lowest}/t_1 and (b) $|\cos \theta|$ as a function of t_2/t_1 . The results are determined by the optimized binary configurations (Binary) and quantum eigensolver (QE) approaches. $|\cos \theta|$ is computed by $|\cos \theta| = \langle \psi^{\text{Exact}} | \psi^{\text{Compare}} \rangle$, where $|\psi^{\text{Compare}}\rangle$ is $|\psi^{\text{Exact}}\rangle$, $|\psi^{\text{Binary}}\rangle$ or $|\psi^{\text{QE}}\rangle$. Here, all eigenstates are normalized.

from QA measurement in (i) procedure. We measure $|\psi\rangle$ in Eq. (2) through QA approach again. Note that $\langle \psi' | \hat{H} | \psi \rangle$ and $\langle \psi' | \hat{H} | \psi \rangle^T$ are only diagonal parts in the matrix of Eq. (2). (iii) Next, $|\psi'\rangle$ is replaced into $|\psi\rangle$ measured in (ii) procedure, and (i) procedure is running again. $|\psi'\rangle$ is no longer $|\psi^{\text{Binary}}\rangle$. (iv) This process is repeated until $|\psi'\rangle$ converges into $|\psi\rangle$ without assistance of derivation on classic computer.

The excited eigenvalue and its $|\psi\rangle$ are determined using the modified Hamiltonian H^{Excited} , which is given by $\hat{H}^{\text{Excited}} = \hat{H} - w|\Psi\rangle\langle\Psi|$, where $|\Psi\rangle$ is the eigenstate of a one-level-lower eigenvalue [18]. We impose an orthonormal condition on $|\psi\rangle$ and $|\Psi\rangle$. w is a constant estimated as $w = h - l$, where h and l are the highest and lowest eigenvalues of \hat{H} , respectively. Finally, the excited E and its $|\psi\rangle$ in \hat{H}^{Excited} are computed using the same optimization method as described in Eq. (1). The computational expense is ηML for the full E and $|\psi\rangle$ of \hat{H} . Notably, L and other parameters in \hat{H} do not significantly affect the computational time, contrary to the ED algorithm with L^3 iterations and GD optimization with $N^2 L^2$ algorithm on a classical computer, because η is a very short time within 10^{-2} seconds for the D-Wave QA.

Hamiltonian for inspection of QE—We selected the one-dimensional ionic $t_1 - t_2$ tight-binding \hat{H} that con-

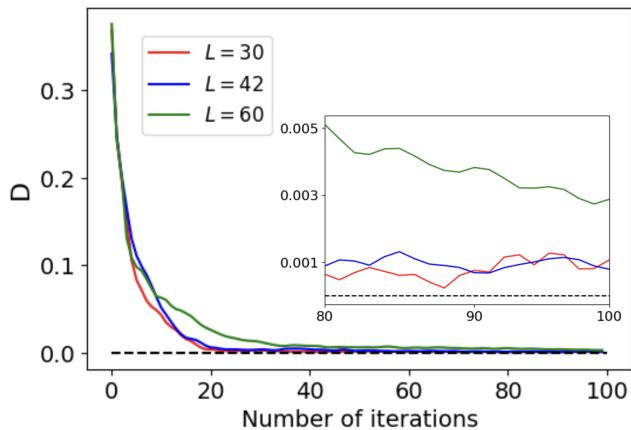


FIG. 3. (Color online) Deviations D as a function of number of iteration for convergence in QE algorithm with different system size L . D are determined by $D = |E^{\text{Exact}} - E^{\text{QE}}|$ at the lowest states with $t_2/t_1 = 1.0$. Inset shows the subtle D after convergence of QA measurements using the QE approach. We confirmed that D were below 5×10^{-3} in all cases.

tains the exact E in all energy states to demonstrate the accuracy and efficiency of our algorithm on the D-Wave QA. The Hamiltonian \hat{H} is given by

$$\hat{H} = -t_1 \sum_{\langle i,j \rangle} (c_i^\dagger c_j + \text{H.C.}) - t_2 \sum_{\langle i,j' \rangle} (c_i^\dagger c_{j'} + \text{H.C.}) + \sum_{i=0}^L \left[\Delta(-1)^{(i)} - \mu \right] n_i, \quad (3)$$

where c_i^\dagger and c_i are the electron creation and annihilation operators at site i , respectively. H.C. is a Hermitian conjugate. t_1 and t_2 are the nearest neighbors at site j and next nearest-neighbor hopping at site j' , respectively. L is the number of lattices under periodic boundary condition. μ and Δ are the chemical and ionic potentials, respectively.

Quantum Annealing Measurements—We used D-Wave QA Advantage2 prototype2.3, where the qubits are designed in a Zephyr structure, for the QA measurements, as shown in Fig. 1 (a). Under Zephyr topology, each qubit is connected to 20 different qubits via a coupler. The architecture of the original \hat{H} (or \hat{H}^{Excited}) topologically matches that of a Zephyr graph by embeddings with chains of ferromagnetic (FM) order between qubits. Here, the embedding Hamiltonian $\hat{H}^{\text{Embedding}}$ is given by $\hat{H}^{\text{Embedding}} = \hat{H} + \hat{H}^{\text{Chain}}$, where \hat{H}^{Chain} is the chain part required for embedding. More qubits are required than in the original ones to form chains. In addition, the elements in the excited \hat{H}^{Excited} are completely occupied. We used the 'dwave.embedding.zephyr.find clique embedding' library provided by D-Wave Ocean Package for embedding of the fully connected systems. Fig. 1 (b) shows the number of qubits as a function of L for the original \hat{H} and $\hat{H}^{\text{Embedding}}$. The optimal chain coupling for

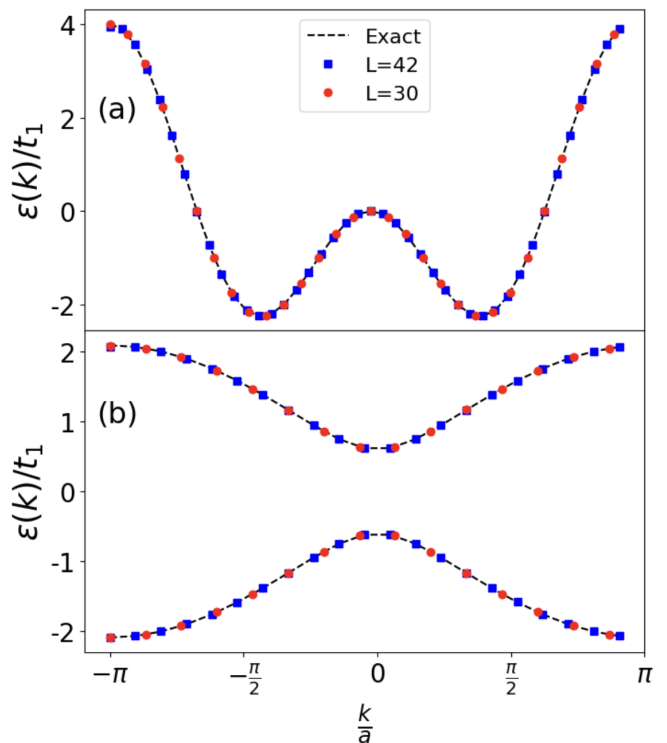


FIG. 4. (Color online) Energy dispersion $\epsilon(\mathbf{k})/t_1$ as a function of momentum k/a for (a) metal with $\Delta/t_1 = 0.0$ and (b) insulator with $t_2/t_1 = 0.0$. Other parameters are $t_2/t_1 = 1.0$ and $\Delta/t_1 = 0.6$ for metal and insulator, respectively. The lattice constant a is set to 1.

an appropriate FM order in the chains was determined using the method proposed by our group. The annealing time was set to 10^{-4} seconds per a QA shot. The total annealing time η with 100 QA shots was set to 10^{-2} seconds.

The lowest eigenvalues and eigenstates on metallic phase—We first measured E^{Lowest} and its $|\psi\rangle$ of \hat{H} with $\Delta = 0.0$ as a function of t_2/t_1 using a QA with optimized binary configurations and QE approaches on the D-Wave QA. E^{Binary} is determined using

$$E^{\text{Binary}} = \min_{|\psi^{\text{Binary}}\rangle} \langle \psi^{\text{Binary}} | \hat{H} | \psi^{\text{Binary}} \rangle. \quad (4)$$

Fig. 2 (a) shows E^{Lowest}/t_1 as a function of t_2/t_1 . From $t_2/t_1 = 0.0$ to $t_2/t_1 = 0.3$, E^{Binary} and E^{QE} are equal to the exact E^{Exact} . After passing through this region, E^{QE} remained equal to E^{Exact} within errors of 5×10^{-3} , whereas E^{Binary} was much higher than E^{Exact} . We also computed $|\cos \theta|$, which is given by the dot product of $|\psi^{\text{Binary}}\rangle$, $|\psi^{\text{QE}}\rangle$ and $|\psi^{\text{Exact}}\rangle$ to confirm the similarity of the eigenstates. Here, $|\psi^{\text{Exact}}\rangle$ was computed by the NumPy library. The results are present in Fig. 2 (b). We confirmed that $|\cos \theta|$ between exact and QE eigenstates is nearly 1. It means that $|\psi^{\text{QE}}\rangle$ and $|\psi^{\text{Exact}}\rangle$ agree well, as indicated by E^{Lowest}/t_1 in Fig. 2 (a).

In Fig. 3 we present the deviations D as a function

of the number of iterations in the QE algorithm for systems with $L = 30, 42$ and 60 at $t_2/t_1 = 1.0$. Here, the deviations D are computed by $D = |E^{\text{Exact}} - E^{\text{QE}}|$. Regardless of L , the convergence condition under which D disappears was satisfied after 50 iterations. It means that only 50×10^{-2} and $L \times 50 \times 10^{-2}$ seconds were enough to reach converged results in the QE algorithm of Eq. (1) and to measure full E^{QE} in all energy states, respectively. The inset of Fig. 3 shows the subtle D observed in the QA measurements using the QE approach, after convergence. We confirmed that D were below 5×10^{-3} in all cases.

Energy dispersion including information of the full eigenvalues of all spectrum—Finally, we computed the energy dispersion $\epsilon(\mathbf{k})$ in two cases with metallic and insulating phases at $\mu = 0.0$, because $\epsilon(\mathbf{k})$ includes E in all energy states in the momentum space. Here, $\epsilon(\mathbf{k})$ are expressed as $\epsilon(\mathbf{k}) = -2t_1 \cos \mathbf{k} - 2t_2 \cos 2\mathbf{k}$ and $\epsilon(\mathbf{k}) = \pm \sqrt{(-2t_1 \cos \mathbf{k})^2 + \Delta^2}$ for metal with $\Delta/t_1 = 0$ and insulator with $t_2/t_1 = 0$. We also employed $t_2/t_1 = 1.0$ and $\Delta/t_1 = 1.0$ for metallic and insulating phases, respectively. Here, \mathbf{k} means the momentum space. The lattice constant a is set to 1. The results of $\epsilon(\mathbf{k})$ that contain the full E values for the entire spectra for the metallic and insulating phases of different L values are shown in Figs. 4(a) and (b), respectively. We confirmed that the E values determined using the QE method exactly match exact $\epsilon(\mathbf{k})$ in both the metallic and insulating phases.

Conclusion—The QA approach only provides $|\psi^{\text{Binary}}\rangle$ and its corresponding E^{Binary} . Thus, an extension of the optimized binary configuration is required to capture $|\psi\rangle$ with continuous variables. We developed a full QE based on iterative QA measurements on the D-Wave QA. The approach adjusted $|\psi\rangle$ correctly from the initial $|\psi^{\text{Binary}}\rangle$ without requiring derivation using a classical computer. The computational cost is ηML for full E and $|\psi\rangle$ for \hat{H} with L . η was set to be below the maximum value of 10^{-2} seconds. Thus, the computational time was not significantly affected by L and M . This differs to the ED algorithm with L^3 iterations and the GD approach with derivations of $N^2 L^2$ on a classical computer. We considered two cases with metallic and insulating phases in the one-dimensional non-interacting ionic tight-binding \hat{H} that contains the exact E in the entire spectra to confirm the efficiency and accuracy of the QE algorithm on D-Wave QA. We determined that the iterations of the QA measurements using the QE method converged well. In addition, we confirmed that the QE method provided an exact E within an error of 5×10^{-3} . Finally, we believe that the proposed QE will not only demonstrate computational supremacy over various numerical approaches on classic computers, but also be widely used for various applications, such as novel material and drug design.

Acknowledgements—This work was supported by Institute of Information and communications Technology Planning Evaluation (IITP) grant funded by

the Korean government (MSIT) (No. RS-2023-0022952422282052750001) and by the quantum computing technology development program of the National Research Foundation of Korea (NRF) funded by the Korean government (Ministry of Science and ICT(MSIT)) (No. 2020M3H3A1110365).

* Email: hplee@kangwon.ac.kr

- [1] A. Weiße and H. Fehske, Exact Diagonalization Techniques, Computational Many- Particle Physics Lecture Notes in Physics, **739**, (2008).
- [2] J. Preskill, Quantum Computing in the NISQ era and beyond, *Quantum* **2**, 79 (2018).
- [3] Oscar Higgott, Daochen Wang, and Stephen Brierley, Variational Quantum Computation of Excited States, *Quantum* **3**, 156 (2019).
- [4] Kishor Bharti, Alba Cervera-Lierta, Thi Ha Kyaw, Tobias Haug, Sumner Alperin-Lea, Abhinav Anand, Matthias Degroote, Hermanni Heimonen, Jakob S. Kottmann, Tim Menke, Wai-Keong Mok, Sukin Sim, Leong-Chuan Kwek, and Alán Aspuru-Guzik, Noisy intermediate-scale quantum algorithms, *Rev. Mod. Phys.* **94**, 015004 (2022).
- [5] Tadashi Kadowaki and Hidetoshi Nishimori, Quantum annealing in the transverse Ising model, *Phys. Rev. E* **58**, 5355 (1998).
- [6] M. W. Johnson, M. H. S. Amin, S. Gildert, T. Lanting, F. Hamze, N. Dickson, R. Harris, A. J. Berkley, J. Johansson, P. Bunyk, et al., Quantum annealing with manufactured spins, *Nature* **473**, 194 (2011).
- [7] A.D. King, S. Suzuki, J. Raymond et al., Coherent quantum annealing in a programmable 2000 qubit Ising chain, *Nature Phys.* **102**, 1745 (2022).
- [8] M.H. Amin, E. Andriyash, J. Rolfe, B. Kulchytsky, and Roger Melko, Quantum Boltzmann Machine, *Phys. Rev. X* **8**, 021050 (2018).
- [9] Inoue, D., Okada, A., Matsumori, T. et al., Traffic signal optimization on a square lattice with quantum annealing, *Sci Rep* **11**, 3303 (2021).
- [10] A. D. King, C. D. Batista, J. Raymond, T. Lanting, I. Ozfidan, G. Poulin-Lamarre, H. Zhang, and M. H. Amin, Quantum Annealing Simulation of Out-of-Equilibrium Magnetization in a Spin- Chain Compound, *PRX Quantum* **2**, 030317 (2021).
- [11] Paul Kairys, Andrew D. King, Isil Ozfidan, Kelly Boothby, Jack Raymond, Arnab Banerjee, and Travis S. Humble, Simulating the Shastry-Sutherland Ising Model Using Quantum Annealing, *PRX Quantum* **1**, 020320 (2020).
- [12] King, A.D., Raymond, J., Lanting, T. et al., Scaling advantage over path-integral Monte Carlo in quantum simulation of geometrically frustrated magnets, *Nat. Commun.* **12**, 1113 (2021).
- [13] H. Park, and H. Lee, Frustrated Ising Model on D-wave Quantum Annealing Machine *J. Phys. Soc. Jpn.* **91**, 074001 (2022).
- [14] Irie, H., Liang, H., Doi, T. et al. Hybrid quantum annealing via molecular dynamics. *Sci Rep* **11**, 8426 (2021).
- [15] Tameem Albash and Daniel A. Lidar, Demonstration of a Scaling Advantage for a Quantum Annealer over Sim-

- ulated Annealing, *Phys. Rev. X* **8**, 031016 (2018).
- [16] V. Kumar, N. Baskaran, V. S. Prasanna, K. Sugisaki, D. Mukherjee, K. G. Dyll, and B. P. Das, Computation of relativistic and many-body effects in atomic systems using quantum annealing, *Phys. Rev. A* **109**, 042808 (2024).
- [17] A. Teplukhin, B. K. Kendrick, S. Tretiak, and P. A. Dub, Electronic structure with direct diagonalization on a D-wave quantum annealer, *Scientific Reports* **10**, 20753 (2020).
- [18] C. F. A. Negre, A. Lopez-Bezanilla, Y. Zhang, P. D. Akrobotu, S. M. Mniszewski, S. Tretiak, and P. A. Dub, Toward a QUBO-Based Density Matrix Electronic Structure Method, *Journal of Chemical Theory and Computation* **18** (7), 4177 (2022).